

**DETECTING SHOCK EFFECTS ON MARS USING MINERAL SPECTROSCOPY.** S. Shkolyar<sup>1,2,3</sup> ([svetlana.shkolyar@nasa.gov](mailto:svetlana.shkolyar@nasa.gov)), S. J. Jaret<sup>4</sup>, B. A. Cohen<sup>2</sup>, J. R. Johnson<sup>5</sup>, A. Ollila<sup>6</sup>, O. Beyssac<sup>7</sup>. <sup>1</sup>USRA, <sup>2</sup>NASA Goddard Space Flight Center, <sup>3</sup>Blue Marble Space Institute of Science, <sup>4</sup>American Museum of Natural History, <sup>5</sup>Applied Physics Laboratory, Johns Hopkins University, <sup>6</sup>Los Alamos National Laboratory, <sup>7</sup>IMPMC, Sorbonne Univ.

**Introduction:** The Mars Sample Return (MSR) campaign begins with the Mars 2020 mission [1,2]. One of the main objectives of the Perseverance mission will be to characterize processes that formed and modified the geologic record for evidence of a habitable environment and geologic diversity within Jezero Crater [3,4]. Lithologies investigated at the landing site will be prioritized for sampling based on their potential to contain evidence of biosignatures and to improve the understanding of Mars' early geologic, geochemical, and climatic evolution.

Impact-induced shock effects may be ubiquitous at Jezero. Shock metamorphism combines the effects of shock wave passage (*e.g.*, solid-state) with subsequent thermal effects (*e.g.*, heating, chemical diffusion) that may negatively affect intended studies of returned samples. Shock effects may reduce the preservation of organic carbon or microtextures within rocks that would help interpret biosignatures. Shock metamorphism may affect geochronology studies of returned samples by altering the boundary conditions of isotopic equilibration and decreasing the time required to reset ages in phases with low diffusion rates [5,6]. Paleomagnetism studies may also be affected by shock metamorphism, potentially impeding our understanding of Martian thermal history and habitability [7-9]. Here, we review shock indicators in feldspars as revealed in spectroscopy lab data and consider implications for MSR sampling decisions.

**Shock Indicators in feldspar:** We are exploring whether shock indicators can be obtained using the Perseverance onboard instrument suite. Here we focus on one Mars-relevant mineral type, plagioclase feldspar, although other shock-related minerals may also be detectable with Perseverance instruments (*e.g.*, high-pressure quartz phases, ringwoodite, phosphates). Impact events result in a range of complex deformation products in feldspar [10, 24]. Impact deformation effects in plagioclase occur as degradation of the crystalline order with increasing shock pressure, from fracturing, to solid-state amorphization, to melting at high pressure [11-15]. Feldspar disordering generally begins at pressures ~15–20 GPa, diaplectic feldspar glass formation occurs at ~25–45 GPa, and significant melting occurs at >~45 GPa [11-13, 16, 17, 35]. The shock pressures at which structural disorder and melting occur are dependent on preshock rock properties (mainly composition, but also porosity, grain size).

**Perseverance Rover Detection:** Shock indicators may be revealed by Raman and luminescence spectroscopy using SuperCam and SHERLOC onboard the Perseverance rover [18]. SuperCam includes time-resolved Raman (532 nm ns-pulsed laser to remove luminescence

and daylight from Raman spectra) and time-resolved luminescence (allowing induced luminescence to be analyzed in the spectrometers in the same region as Raman) [19, 20]. Spectral ranges are 150–4400  $\text{cm}^{-1}$  (Raman) and ~536–850 nm (luminescence). SHERLOC is a Deep UV (DUV) resonance Raman and fluorescence spectrometer utilizing a 248.6-nm DUV laser. SHERLOC's Raman spectral range is 800 to >3600  $\text{cm}^{-1}$  and its fluorescence spectral window is 250–360 nm [21]. Both SuperCam and SHERLOC are equipped with microimagers for target documentation.

Raman spectroscopy is a vibrational spectroscopic technique measuring inelastic scattering. The technique is sensitive to low-frequency lattice modes and crystallinity in mineral crystals, making it ideal to characterize shock in feldspars [15, 22–24]. With increased shock pressure, Raman spectral observations of albite, andesine, and bytownite generally reveal (1) decreased intensities or disappearance of characteristic peaks at 514  $\text{cm}^{-1}$  and 1000  $\text{cm}^{-1}$ , (2) broadening and convergence of 1000–1060  $\text{cm}^{-1}$  and 400–500  $\text{cm}^{-1}$  features, (3) appearance of peaks, and (4) shifts in some peaks to higher wavenumbers (when measured under pressure) [5, 15, 22–28]. See Fig. 1 for examples within SuperCam's spectral range. With increasing amorphization, peaks often converge and broaden, too [22, 24]. Sometimes, peak intensity and FWHM decrease at high pressures and background luminescence increases, seen as a broad hump in a Raman spectrum [13, 15, 17, 29]. Additional Raman-based parameters (*e.g.* peak ratios) also correlate moderately with increasing shock but may not be systematic [5, 15, 28, 30, 35].

Luminescence features can be seen in feldspars due to either shock-induced lattice defect centers or cation substitutions with changing mineral structure. With increasing shock, luminescence intensity (measured as cathodoluminescence spectra in the lab) and peak wavelength are thought to depend on shock pressures, rather than in-shock and post-shock temperatures during impacts [30, 31]. Shock-induced band changes in plagioclase glasses at 550 nm, 660 nm, 720, 750, and 770 nm can be attributed to the lattice defects in K-, Na-, and Ca-feldspars in the Al and Si structure and by distortion or dislocation of the Si and Al octahedral structure [31]. Features appearing at 715–730 nm can be caused by  $\text{Fe}^{3+}$  or  $\text{Mn}^{2+}$  impurity centers substituting for  $\text{Al}^{3+}$  tetrahedral sites in shocked plagioclase [26,31], shifting or diminishing with shock pressure if coordination configuration around  $\text{Mn}^{2+}$  is changed [31]. Fig. 2 illustrates an example in SuperCam's spectral range. Optically stimulated luminescence (OSL) [32, 33] may be measurable with SHERLOC [34] and the WATSON CCD, but this

technique is currently in a very immature state.

In addition, studies of the effects of shock on feldspars using IR spectroscopy have been performed [e.g., 17, 35]. Most focused on thermal IR, relevant to other planetary applications, but not Perseverance (SuperCam is confined to the near IR, 0.4 - 2.6 microns). Shock effects in this range are less explored. One study [17] suggests that shock effects may be detectable at high shock levels, but are less obvious than those in the thermal IR.

**Conclusions:** Shock-induced spectral features may be detectable in feldspar with the spectral techniques available onboard Perseverance. However, major challenges may prevent confident spectral shock identification with Raman or luminescence. They include unambiguous mineral identification, mineral composition, grain size, and instrument spot size. Many spectral parameters related to shock effects are only moderately correlated to shock levels given optimized sampling conditions in a lab setting and are likely less so in a rover setting. Also, SHERLOC's Raman and luminescence spectral ranges are largely out of range of many features associated with shock in feldspars (Figs. 1 and 2).

Several recommendations can also be made to inform MSR decisions on Mars. Rather than examining samples using individual spectral peaks, shock level assessment may involve assessing their standard deviations. Standard deviations of peaks at increasing pressures have been used to gauge how accurately certain techniques can be quantitative indicators shock [5, 28, 31, 35] and should be investigated further. Also, Raman data alone is limited as a shock barometer and should be complimented with chemical data on the same samples.

**References:** [1] Farley K. A., et al. (2020) *Space Sci. Rev.* 216(8), 142. [2] Paul A. B. and Carlos E. S. (2020) In *Proc. SPIE*. [3] Ehlmann B. L., et al. (2008) *Science* 322, 1828-1832. [4] Goudge T. et al. (2018) *Icarus* 301, 58-75. [5] Jaret S. J., et al. (2018) *EPSL* 501, 78-89. [6] Nyquist L. E., et al. (1987) *LPS XVIII*, 732-733. [7] Halls H. C. (1979) *Geophys J International* 59(3), 553-591. [8] Rochette P., et al. (2003) *GRL* 30(13). [9] Tikoo S. M., et al. (2015) *JGR: Planets* 120(9), 1461-1475. [10] Pickersgill, A., et al. (2021) *GSA Special Papers*, in press. [11] D. Stöffler (1971) *Fortschritte der Mineralogie* 49, 50-113. [12] R. Ostertag (1983) *JGR: Solid Earth* 88, B364-B376. [13] D. Heymann and F. Hörz (1990) *Phys Chem Min* 17, 38. [14] D. Stöffler, D. et al. (1991) *GCA*, 55(12), 3845-3867. [15] J. Fritz, A. Greshake, and D. Stöffler (2005) *Antarctic Meteorite Research* 18, 96. [16] Bunch T. E., et al. (1967) *The American Mineralogist*, 52, 244-253. [17] J.R. Johnson and F. Hörz (2003) *JGR: Planets*, 108. [18] Caffrey M., et al. (2020) *2020 IEEE*, 1-8. [19] Wiens, R.C., et al. (2020) *Space Sci. Rev.* 217, 4. [20] Maurice, S., et al. (2020) *Space Sci. Rev.* 217, SPAC-D-20-00069R1. [21] Bhartia, R. et al. (2020) *Space Sci. Rev.* [22] B. Velde, et al. (1989) *Phys Chem Min*, 16, 436-441. [23] Jaret, S. J., et al. (2014) *MPS*, 49(6), 1007-1022. [24] Jaret, S. J.,

et al. (2015) *JGR: Planets*, 120(3), 570-587. [25] J. J. Freeman, A. et al. (2008) *Canadian Mineralogist* 46, 1477-1500. [26] M. Kayama, et al. (2009) *American Institute of Physics Conference Proceedings*, p. 86. [27] K. Befus, et al. (2018) *Amer Mineralogist: Journal of Earth and Planetary Materials* 103, 600-609. [28] J. R. Johnson, et al. (2020) *JGR: Planets*, 125. [29] L. Pittarello, et al. (2020) *MPS*, 55, 669-678. [30] I. P. Baziotis, et a. (2013) *Nature Comm* 4, 1-7. [31] M. Kayama, H. et al (2012) *JGR: Planets* 117. [32] Smith et al. (1986), *Rad Protection Dosimetry* 17, 229-233. [33] M. Jain, et al. (2006) *Rad Measurements* 41, 755-761. [34] K. H. Williford, et al. (2018) *From Habitability to Life on Mars*, 275-308. [35] Jaret, S.J. et al. (2018) *JGR*, 123, 2018EJ005523.

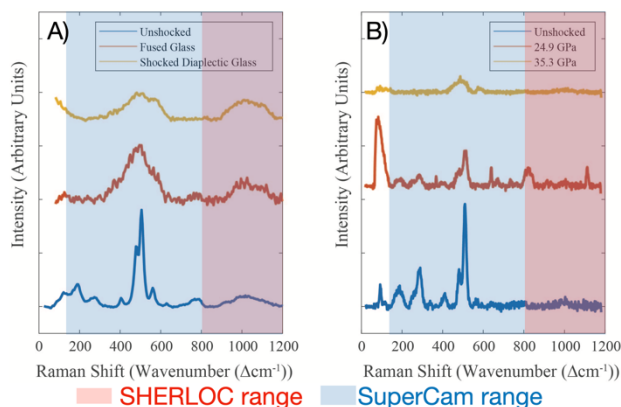


**Fig. 1.** Raman spectra of natural and experimentally amorphized feldspars. **A)** Comparison of crystalline (blue), shocked (yellow), and fused (red) labradorite from ref. 24. **B)** Crystalline and experimentally shocked andesine from ref. 35, revealing decreased peak intensities with increasing shock. Crystalline and glassy phases are easily distinguished but types (shock or fused) are not. SuperCam and SHERLOC spectral ranges are shown.

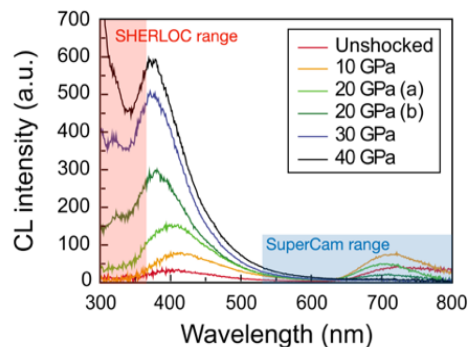


**Fig. 2.** Experimentally shocked sanidine cathodoluminescence spectra (modified from [31]). Band intensity changes and shifts at 715 - 720 nm (based on composition) indicate a  $Mn^{2+}$  impurity center coordinate configuration change and decreased crystal field strength. SuperCam and SHERLOC spectral ranges are shown.